Computer Chemistry

Green Oxidation Catalysts: Computational Design of High-Efficiency Models of Galactose Oxidase**

*Leonardo Guidoni, Katrin Spiegel, Martin Zumstein, and Ursula Röthlisberger**

The metalloenzyme galactose oxidase (GOase) is a highly efficient catalyst for the two-electron oxidation of a broad variety of primary alcohols. This enzyme is capable of catalytic oxidations in water, making direct use of the molecular oxygen of the air. Even polyalcohols are converted, in a highly regio and stereoselective way, into the corresponding aldehydes. This elegant synthetic route stands out against the stoichiometric alternatives of the same reaction as performed by traditional inorganic oxidants. Not surprisingly, GOase thus constitutes a highly attractive target for the development of biomimetic strategies aimed at the design of environmentally friendly, green oxidation catalysts.[1] During the last years, this enzyme has inspired a variety of groups to design synthetic analogues. Although different classes of spectroscopic,[2] structural[3] and even functional[4–9] models of GOase have been characterized, none of them is as yet able to compete with the natural enzyme in terms of catalytic efficiency. For the few existing functional models, rates of turnover lie still approximately four orders of magnitude

[*] Dr. L. Guidoni, K. Spiegel,[+] M. Zumstein, Prof. Dr. U. Röthlisberger
Institut de chimie moléculaire et biologique
Ecole polytechnique fédérale de Lausanne—BCH—LCBC
1015 Lausanne (Switzerland)
Fax: (+41) 21-693-0320
E-mail: ursula.roethlisberger@epfl.ch

[+] Present address:
Statistical and Biological Physics Sector
International School for Advanced Studies
Via Beirut, 4 34014, Trieste (Italy)

[**] We are grateful to the Swiss Center for Scientific Computing (Large User Project Grant 2002–2003) for providing computational resources. We thank Prof. H. Grützmacher for stimulating discussions and comments to the manuscript.

Supporting information for this article is available on the WWW under http://www.angewandte.org or from the author.

  DOI: 10.1002/anie.200454081

below that of the natural target (around 0.5 s^{-1} [10] versus 800 s^{-1} for GOase[11]).

How does the enzyme achieve this remarkable proficiency and in which way do the synthetic analogues differ from their natural counterpart? Numerous investigations have contributed to a basic understanding of the enzymatic mechanism of action. [11–14] These studies have confirmed that GOase applies an intricate type of radical chemistry in which the metal ion serves as a one-electron redox center whereas the second electron is provided by a protein radical site. The enzyme contains a copper ion in an approximately square-pyramidal coordination environment with two nitrogen and two oxygen equatorial donor atoms (originating from His581, His496, Tyr272 and the substrate) with an additional oxygen atom from an axial ligand (Tyr495) as depicted in Scheme 1. As a peculiar feature, the equatorial Tyr272 shows an unusual covalent linkage to Cys228. In the active form, the unpaired spin of a copper(II) ion is antiferromagnetically coupled to a tyrosyl radical, thus forming an EPR-silent, open-shell singlet complex.[15,16] As a first step of the catalytic process (**A**→**B**), an alcoholate is formed through the deprotonation of the substrate by the axial tyrosinate ligand acting as a general base. In the next reaction step (**B**→**C**), a hydrogen atom is abstracted from the substrate to the equatorial tyrosyl radical (**C**→**D**) and subsequently (or quasi simultaneously) the copper center is reduced to Cu^{I} by a single-electron transfer from the ketyl radical (**D**→**E**). The weakly bound newly formed aldehyde is replaced by dioxygen and the catalytic cycle is closed by recovering the initial copper oxidation state under concomitant reduction of O_2 to H_2O_2 (**E**→**A**). Measurements of the kinetic isotope effect reveal that the H-abstraction step is rate-limiting for substrates that are more difficult to oxidize.[13]

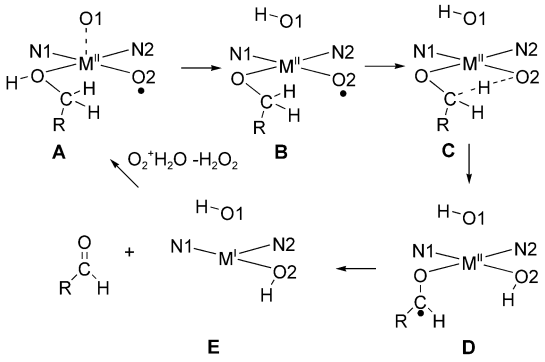

Scheme 1. Simplified reaction mechanisms of GOase and its models.

Notwithstanding the fact that the recently developed functional models of GOase apparently reproduce the overall features of the natural reaction (e.g., an EPR-silent active form and a kinetic isotope effect of similar magnitude[4]) they fail to rival the natural activity.

A number of recent quantum-chemical investigations have aimed at a full atomistic characterization of the enzymatic reaction mechanism, thereby complementing the available experimental data.[16–19] We have recently performed a mechanistic analysis of the functional biomimetic compound developed by Wang et al.[4] (MIM0 in Scheme 2)[18] in direct comparison with its natural target.[17] This study identified the delocalization of the unpaired spin density during the rate-determining H-abstraction step (Scheme 1, **C**→**D**) as the crucial determinant for the efficiency of the process. Specifically, due to a different orientation of the equatorial tyrosyl ligand (in MIM0 the equatorial ring system is essentially in plane with the copper coordination plane, whereas in GOase it is almost perpendicular) the spin delocalization in the transition state is greatly reduced in the synthetic compound. A second relevant difference concerns the product release step (Scheme 1, **D**→**E**). In the case of MIM0 the copper centre loses one of its nitrogen ligands to adopt a competing conformation in which the phenolate-binaphtyl moiety is fully planar and thus stabilized by hyperconjugation. Consequently, the newly formed aldehyde is strongly bound and cannot be released as easily as in the case of GOase, in which it is only marginally coordinated to the copper ion. These crucial factors identified in our previous study, namely: 1) efficient spin delocalization in the rate-determining transition state; 2) stabilization of the copper coordination sphere in the product-release step can now be used as a guideline for the design of modified synthetic models with increased activity. Herein, in particular, we probe the effects of alternative metal centers, ligand modifications, and group substitutions, with the aim of designing more efficient compounds with accessible synthetic strategies.

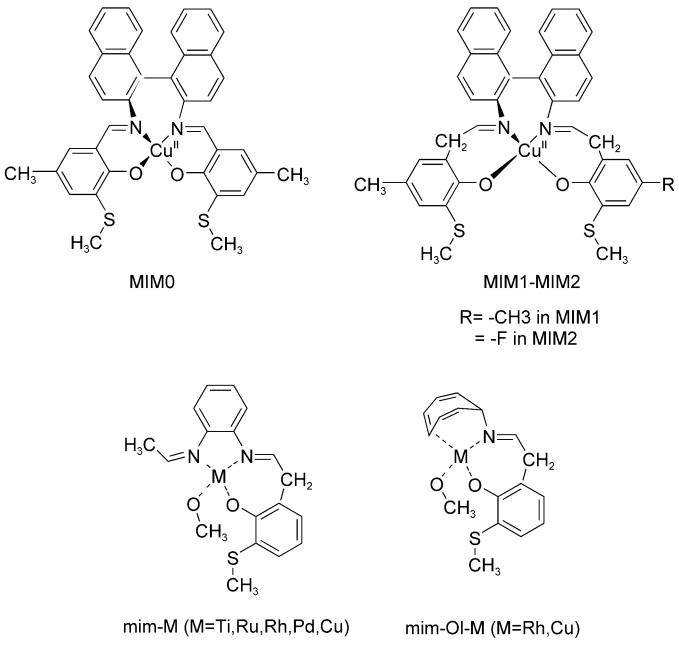

Scheme 2. Full (MIM- top) and minimal (mim- bottom) computational models used in our calculations.

Ligand Modifications: We designed two new biomimetic models derived from MIM0 (see Scheme 2): in MIM1, we introduced an additional CH_2-group between the phenolate and the binaphtyl moiety to break the extended conjugated system and to introduce more flexibility for an optimal orientation of the equatorial ring. In MIM2, we also

introduced a fluorine atom in the *para* position of the critical equatorial ring to enhance the spin delocalization from the copper center and the substrate towards the equatorial ligand.[18]

As intended, the enhanced flexibility introduced by the additional -CH_2 group leads to a different orientation of the aromatic ring of the equatorial phenolate ligand. In the reactant geometries (Scheme 1 **B**) the aromatic ring moves significantly out of the coordination plane, with an angle between the aromatic ring system and the copper plane ranging from 55° to 83° (with respect to 21° for MIM0) thus approaching the orientation of the natural system of 71°. Consequently, at the transition state (Scheme 1 **C**), the unpaired spin density of the ketyl radical is partially delocalized to the equatorial tyrosyl. This enhanced delocalization of the unpaired spin density in the transition state has indeed a distinct effect on the activation barrier.[18] The enzymatic activation barrier has been estimated from experimental turnover rates to be about 14 kcal mol^{-1}.[11] Within our computational framework,[*] we previously obtained an activation barrier for GOase and MIM0 of 16 and 21 kcal mol^{-1}, respectively.[18] The structural modifications introduced in the design of MIM1 and MIM2 are able to reduce the activation barrier significantly resulting in values as low as 13.8 kcal mol^{-1} for the case of MIM2, that is, a value even lower than that for the natural enzyme (Table 1). The expected turn over rates for MIM1 and MIM2 are 150 s^{-1} and 4000 s^{-1}, respectively, therefore up to five orders of magnitude higher than the one of the original compound MIM0.

Table 1: Activation barriers for GOase and its models.

Catalyst	GOase	MIM0	MIM1	MIM2	mim-Cu	mim-Ol-Cu	mim-Rh	mim-Ol-Rh
Activation barrier [kcal mol^{-1}]	16.0	21.0	15.7	13.8	15.8	14.1	22.9	21.4

For a more complete scan of optimal modified ligand systems and possible metal substitutions, we also developed a smaller computational model that is able to catch the essential features of MIM1 and MIM2 at a lower computational cost. To this purpose, we investigated the H-abstraction step of the minimal compound mim-Cu (see Scheme 2), and found excellent similarity to MIM1 in terms of geometry and activation energy as shown in Table 1. The axial ligand seems, therefore, not to be important for H-abstraction and matter only for the protonation/deprotonation steps. The robustness of our scaffold against ligand substitutions has been further investigated by replacing the phenylamine-*N*-ethylidene with a seven membered olefine ring (mim-Ol-Cu in Scheme 2). Again, in this case, the calculated activation barrier turns out to be insensitive to this substitution.

Alternative Metals: With the aim of investigating whether these catalytic properties are unique to copper, we also explored the possibility of using alternative metal centers. From the experimental point of view, the search for alternative transition metal centers in functional models of GOase has so far been limited to Zn^{II},[8] however, with inferior turnover rates (0.02 s^{-1} for Cu^{II} vs 0.003 s^{-1} for Zn^{II}). As a further alternative, herein, we concentrate our studies on compounds based on the Rh^{I}/Rh^{II} center (mim-Rh and mim-Ol-Rh in Scheme 2).[+]

The calculated activation barrier for mim-Rh and mim-Ol-Rh are 22.7 and 21.4 kcal mol^{-1}, respectively, that is, essentially competitive with the one of the copper-containing compound MIM0 (21.0 kcal mol^{-1}). A comparative study of the hydrogen abstraction step in mim-Cu and mim-Rh reveals that although the activation energies are roughly comparable, qualitative differences are present in the electronic structure of the two enzyme mimetics at the transition state. The total integrated spin density is reported as a function of the reaction coordinate in Figure 1 a. These data show that in the case of mim-Rh the electron transfer from the ketyl species to the rhodium ion occurs before hydrogen abstraction (i.e., formally corresponding to a transferred H^+) and not after as in mim-Cu, MIM0, MIM1, and MIM2. At the mim-Rh transition state, the unpaired electron is shared between the substrate and the metal center, in contrast to what occurs in mim-Cu, in which the electron is localized on the substrate and on the equatorial ligand. This difference suggests that, whereas for the copper-based mimetic the reaction is enhanced by improving spin delocalization (to the equatorial ligand), in the case of rhodium a tailoring of the metal redox properties appears to be an apt procedure to lower the rate-limiting barrier.

In summary, we have illustrated how the rational design of modifications of enzyme mimetic compounds can significantly improve their catalytic efficiency, reaching and even surpassing the one of the natural target. Furthermore, other metals, such as rhodium, could replace copper as the redox center, which may result in activation barriers comparable to those found in existing copper-based compounds.

Experimental Section

Methods: Density functional theory calculations were carried out by using the programs CPMD (www.cpmd.org)[20] and ADF[21] with the BLYP exchange correlation functional.[22,23] Geometries were converged up to a residual nuclear gradient of 0.001 atomic units. In CPMD calculations, the Kohn–Sham orbitals were expanded in plane waves with an energy cutoff of 80 Ry, which has been shown to be

[*] The calculations presented here refer to $\Delta U^{\neq}$ which should be a good approximation of $\Delta F^{\neq}$ in the case of a unimolecular reaction with only very minor structural rearrangements.

[+] Preliminary screening within the simplified class of models mim-M (Scheme 2) has also been performed on the series of transition metals M = Ti, Ru, Rh, Pd that were selected because of their similarity to copper in terms of chemical properties (such as redox potential, coordination geometry and ionic radii). The ruthenium and titanium oxidation states involved in the catalytic cycle were Ru^{III}/Ru^{II} and Ti^{IV}/Ti^{III} respectively. Metal-binding energies are reported in the Supporting Information. Whereas Ti favors geometries with an enhanced coordination number, Ru and Pd appear both as valuable alternatives to Rh as reactive centers.

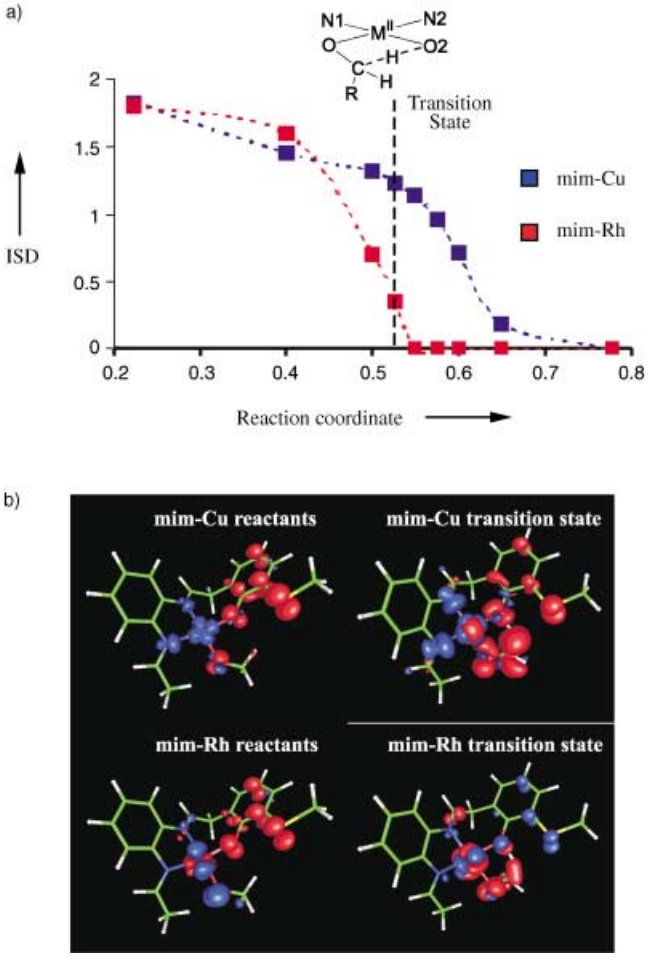

Figure 1. Hydrogen-abstraction step in copper- and rhodium-based models. a) The values of the integrated spin densitiy (ISD) indicate the number of unpaired electrons along the reaction coordinate. Whereas in the case of copper, the electron transfer from the substrate is not completed at the transition state, in the case of rhodium it occurs before hydrogen abstraction. This fact is reflected in the spatial distribution of the unpaired spin density on the substrate radical (b). In mim-Cu (top) the negative charge that accumulates on the substrate during the hydrogen-abstraction step is efficiently delocalized over the phenolate ligand. This stabilizing delocalization is lacking in the case of mim-Rh (bottom).

sufficiently accurate for these compounds.[17] In ADF calculations we used DZP (H, N, O) and TZP (Cu, Ti, Ru, Rh, Pd) basis sets. The transition states of the hydrogen abstraction step have been localized in CPMD by using the three-point constraint described by Ensing et al.[24] on atoms C, H, and O2 (Scheme 1).

Supporting Information includes: the calculated binding energies for mim-M, the coordinates of the fully optimized equilibrium and transition state geometries of mim-Rh and mim-Cu.

Received: February 23, 2004
Revised: April 13, 2004 [Z54081]

Keywords: ab initio calculations · alcohols · biomimetic synthesis · oxidation · transition metals

[1] R. A. Sheldon, I. W. C. E. Arends, G. J. Ten Brink, A. Dijksman, *Acc. Chem. Res.* **2002**, *35*, 774–781.
[2] M. A. Halcrow, L. M. L. Chia, X. M. Liu, E. J. L. McInnes, L. J. Yellowlees, F. E. Mabbs, I. J. Scowen, M. McPartlin, J. E. Davies, *J. Chem. Soc. Dalton Trans.* **1999**, 1753–1762.
[3] Y. Shimazaki, S. Huth, A. Odani, O. Yamauchi, *Angew. Chem.* **2000**, *112*, 1732–1735; *Angew. Chem. Int. Ed.* **2000**, *39*, 1666–1669.
[4] Y. Wang, J. L. DuBois, B. Hedman, K. O. Hodgson, T. D. Stack, *Science* **1998**, *279*, 537–540.
[5] R. Pratt, T. D. P. Stack, *J. Am. Chem. Soc.* **2003**, *125*, 8716–8717.
[6] P. Chaudhuri, M. Hess, U. Flörke, K. Wieghardt, *Angew. Chem.* **1998**, *110*, 2340–2343; *Angew. Chem. Int. Ed.* **1998**, *37*, 2217–2220.
[7] S. Itoh, M. Taki, S. Takayama, S. Nagatomo, T. Kitagawa, N. Sakurada, R. Arakawa, S. Fukuzumi, *Angew. Chem.* **1999**, *111*, 2944–2946; *Angew. Chem. Int. Ed.* **1999**, *38*, 2774–2776.
[8] P. Chaudhuri, M. Hess, J. Muller, K. Hildenbrand, E. Bill, T. Weyhermuller, K. Wieghardt, *J. Am. Chem. Soc.* **1999**, *121*, 9599–9610.
[9] F. Thomas, G. Gellon, I. G. Luneau, E. Saint-Aman, J. L. Pierre, *Angew. Chem.* **2002**, *114*, 3173–3176; *Angew. Chem. Int. Ed.* **2002**, *41*, 3047–3050.
[10] P. Chaudhuri, M. Hess, T. Weyhermüller, K. Wieghardt, *Angew. Chem.* **1999**, *111*, 1165–1168; *Angew. Chem. Int. Ed.* **1999**, *38*, 1095–1098.
[11] R. M. Wachter, B. P. Branchaud, *Biochim. Biophys. Acta* **1998**, *1384*, 43–54.
[12] A. J. Baron, C. Stevens, C. Wilmot, K. D. Seneviratne, V. Blakeley, D. M. Dooley, S. E. V. Phillips, P. Knowles, M. J. Mc. Pherson, *J. Biol. Chem.* **1994**, *269*, 25095–25105.
[13] M. M. Whittaker, D. P. Ballou, J. W. Whittaker, *Biochemistry* **1998**, *37*, 8426–8436.
[14] J. W. Whittaker, *Chem. Rev.* **2003**, *103*, 2347–2363.
[15] J. Müller, T. Weyhermüller, E. Bill, P. Hildebrandt, L. Ould-Moussa, T. Glaser, K. Wieghardt, *Angew. Chem.* **1998**, *110*, 637–640; *Angew. Chem. Int. Ed.* **1998**, *37*, 616–619.
[16] F. Himo, L. A. Eriksson, F. Maseras, P. E. M. Siegbahn, *J. Am. Chem. Soc.* **2000**, *122*, 8031–8036.
[17] U. Rothlisberger, P. Carloni, *Int. J. Quantum Chem.* **1999**, *73*, 209–218.
[18] U. Rothlisberger, P. Carloni, K. Doclo, M. Parrinello, *J. Biol. Inorg. Chem.* **2000**, *5*, 236–250.
[19] L. Guidoni, P. Maurer, S. Piana, U. Rothlisberger, *Quant. Struct. Act. Relat.* **2002**, *21*, 173–181.
[20] CPMD V3.7 Copyright IBM Corp 1990–2003, Copyright MPI fuer Festkoerperforschung Stuttgart, **1997**.
[21] G. T. Velde, F. M. Bickelhaupt, E. J. Baerends, C. F. Guerra, S. J. A. Van Gisbergen, J. G. Snijders, T. Ziegler, *J. Comput. Chem.* **2001**, *22*, 931–967.
[22] A. D. Becke, *Phys. Rev. A* **1988**, *38*, 3098–3100.
[23] C. L. Lee, W. Yang, R. G. Parr, *Phys. Rev. B* **1988**, *37*, 785–789.
[24] B. Ensing, E. J. Meijer, P. E. Blochl, E. J. Baerends, *J. Phys. Chem. A* **2001**, *105*, 3300–3310.

